Seismic analysis of a concrete gravity dam

This example illustrates a typical application of the concrete damaged plasticity material model for the assessment of the structural stability and damage of concrete structures subjected to arbitrary loading.

We consider an analysis of the Koyna dam, which was subjected to an earthquake of magnitude 6.5 on the Richter scale on December 11, 1967. This problem is chosen because it has been extensively analyzed by a number of investigators, including Chopra and Chakrabarti (1973), Bhattacharjee and Léger (1993), Ghrib and Tinawi (1995), Cervera et al. (1996), and Lee and Fenves (1998).

This page discusses:

Products: Abaqus/Standard Abaqus/Explicit

Problem description

The geometry of a typical non-overflow monolith of the Koyna dam is illustrated in Figure 1. The monolith is 103 m high and 71 m wide at its base. The upstream wall of the monolith is assumed to be straight and vertical, which is slightly different from the real configuration. The depth of the reservoir at the time of the earthquake is h_w = 91.75 m. Following the work of other investigators, we consider a two-dimensional analysis of the non-overflow monolith assuming plane stress conditions. The finite element mesh used for the analysis is shown in Figure 2. It consists of 760 first-order, reduced-integration, plane stress elements (CPS4R). Nodal definitions are referred to a global rectangular coordinate system centered at the lower left corner of the dam, with the vertical *y*-axis pointing in the upward direction and the horizontal *x*-axis pointing in the downstream direction. The transverse and vertical components of the ground accelerations recorded during the Koyna earthquake are shown in Figure 3 (units of g = 9.81 m sec^{-2}). Prior to the earthquake excitation, the dam is subjected to gravity loading due to its self-weight and to the hydrostatic pressure of the reservoir on the upstream wall.

For the purpose of this example we neglect the dam–foundation interactions by assuming that the foundation is rigid. The dam–reservoir dynamic interactions resulting from the transverse component of ground motion can be modeled in a simple form using the Westergaard added mass technique. According to Westergaard (1933), the hydrodynamic pressures that the water exerts on the dam during an earthquake are the same as if a certain body of water moves back and forth with the dam while the remainder of the reservoir is left inactive. The added mass per unit area of the upstream wall is given in approximate form by the expression $\frac{7}{8}\rho_w\sqrt{h_w\left(h_w-y\right)}$, with $y \leq h_w$, where ρ_w = 1000 kg/m^3 is the density of water. In the Abaqus/Standard analysis the added mass approach is implemented using a simple 2-node user element that has been coded in user subroutine UEL. In the Abaqus/Explicit analysis the dynamic interactions between the dam and the reservoir are ignored.

The hydrodynamic pressures resulting from the vertical component of ground motion are assumed to be small and are neglected in all the simulations.

Material properties

The mechanical behavior of the concrete material is modeled using the concrete damaged plasticity constitutive model described in Concrete Damaged Plasticity and Damaged plasticity model for concrete and other quasi-brittle materials. The material properties used for the simulations are given in Table 1 and Figure 4. These properties are assumed to be representative of the concrete material in the Koyna dam and are based on the properties used by previous investigators. In obtaining some of these material properties, a number of assumptions are made. Of particular interest is the calibration of the concrete tensile behavior. The tensile strength is estimated to be 10% of the ultimate compressive strength (σ_{cu} = 24.1 MPa), multiplied by a dynamic amplification factor of 1.2 to account for rate effects; thus, σ_{t0} = 2.9 MPa. To avoid unreasonable mesh-sensitive results due to the lack of reinforcement in the structure, the tensile postfailure behavior is given in terms of a fracture energy cracking criterion by specifying a stress/displacement curve instead of a stress-strain curve, as shown in Figure 4(a). This is accomplished with the postcracking stress/displacement curve. Similarly, tensile damage, d_t, is specified in tabular form as a function of cracking displacement by using the postcracking damage displacement curve. This curve is shown in Figure 4(b). The stiffness degradation damage caused by compressive failure (crushing) of the concrete, d_c, is assumed to be zero.

Damping

It is generally accepted that dams have damping ratios of about 2–5%. In this example we tune the material damping properties to provide approximately 3% fraction of critical damping for the first mode of vibration of the dam. Assuming Rayleigh stiffness proportional damping, the factor β required to provide a fraction ξ_1 of critical damping for the first mode is given as $\beta = 2\xi_1/\omega_1$. From a natural frequency extraction analysis of the dam the first eigenfrequency is found to be ω_1 = 18.61 rad sec^{-1} (see Table 2). Based on this, β is chosen to be 3.23 × 10^{-3} sec.

Loading and solution control

Loading conditions and solution controls are discussed for each analysis.

Abaqus/Standard analysis

Prior to the dynamic simulation of the earthquake, the dam is subjected to gravity loading and hydrostatic pressure. In the Abaqus/Standard analysis these loads are specified in two consecutive static steps, using a distributed load with the load type labels GRAV (for the gravity load) in the first step and HP (for the hydrostatic pressure) in the second step. For the dynamic analysis in the third step the transverse and vertical components of the ground accelerations shown in Figure 3 are applied to all nodes at the base of the dam.

Since considerable nonlinearity is expected in the response, including the possibility of unstable regimes as the concrete cracks, the overall convergence of the solution in the Abaqus/Standard analysis is expected to be non-monotonic. In such cases automatically setting the time incrementation parameters is generally recommended to prevent premature termination of the equilibrium iteration process because the solution may appear to be diverging. The unsymmetric matrix storage and solution scheme is activated by specifying an unsymmetric equation solver for the step. This is essential for obtaining an acceptable rate of convergence with the concrete damaged plasticity model since plastic flow is nonassociated. Automatic time incrementation is used for the dynamic analysis of the earthquake, with the half-increment residual tolerance set to 10^7 and a maximum time increment of 0.02 sec.

Abaqus/Explicit analysis

While it is possible to perform the analysis of the pre-seismic state in Abaqus/Explicit, Abaqus/Standard is much more efficient at solving quasi-static analyses. Therefore, we apply the gravity and hydrostatic loads in an Abaqus/Standard analysis. These results are then imported into Abaqus/Explicit to continue with the seismic analysis of the dam subjected to the earthquake accelerogram. We still need to continue to apply the gravity and hydrostatic pressure loads during the explicit dynamic step. In Abaqus/Explicit gravity loading is specified in exactly the same way as in Abaqus/Standard. The specification of the hydrostatic pressure, however, requires some extra consideration because this load type is not currently supported by Abaqus/Explicit. Here we apply the hydrostatic pressure using user subroutine `VDLOAD`.

The Abaqus/Explicit simulation requires a very large number of increments since the stable time increment (6×10^{-6} sec) is much smaller than the total duration of the earthquake (10 sec). The analysis is run in double precision to prevent the accumulation of round-off errors. The stability limit could be increased by using mass scaling; however, this may affect the dynamic response of the structure.

For this particular problem Abaqus/Standard is computationally more effective than Abaqus/Explicit because the earthquake is a relatively long event that requires a very large number of increments in Abaqus/Explicit. In addition, the size of the finite element model is small, and the cost of each solution of the global equilibrium equations in Abaqus/Standard is quite inexpensive.

Results and discussion

The results for each analysis are discussed in the following sections.

Abaqus/Standard results

The results from a frequency extraction analysis of the dam without the reservoir are summarized in Table 2. The first four natural frequencies of the finite element model are in good agreement with the values reported by Chopra and Chakrabarti (1973). As discussed above, the frequency extraction analysis is useful for the calibration of the material damping to be used during the dynamic simulation of the earthquake.

Figure 5 shows the horizontal displacement at the left corner of the crest of the dam relative to the ground motion. In this figure positive values represent displacement in the downstream direction. The crest displacement remains less than 30 mm during the first 4 seconds of the earthquake. After 4 seconds, the amplitude of the oscillations of the crest increases substantially. As discussed below, severe damage to the structure develops during these oscillations.

The concrete material remains elastic with no damage at the end of the second step, after the dam has been subjected to the gravity and hydrostatic pressure loads. Damage to the dam initiates during the seismic analysis in the third step. The evolution of damage in the concrete dam at six different times during the earthquake is illustrated in Figure 6, Figure 7, and Figure 8. Times t_1 = 3.96 sec, t_3 = 4.315 sec, and t_5 = 4.687 sec correspond to the first three large excursions of the crest in the upstream direction, as shown in Figure 5. Times t_2 = 4.163 sec and t_4 = 4.526 sec correspond to the first two large excursions of the crest in the downstream direction. Time t_6 = 10 sec corresponds to the end of the earthquake. The figures show the contour plots of the tensile damage variable, DAMAGET (or d_t), on the left, and the stiffness degradation variable, SDEG (or *d*), on the right. The tensile damage variable is a nondecreasing quantity associated with tensile failure of the material. On the other hand, the stiffness degradation variable can increase or decrease, reflecting the stiffness recovery effects associated with the opening/closing of cracks. Thus, assuming that there is no compressive damage ($d_c = 0$), the combination $d_t > 0$ and $d > 0$ at a given material point represents an open crack, whereas $d_t > 0$ and $d = 0$ represents a closed crack.

At time t_1, damage has initiated at two locations: at the base of the dam on the upstream face and in the region near the stress concentration where the slope on the downstream face changes.

When the dam displaces toward the downstream direction at time t_2, the damage at the base leads to the formation of a localized crack-like band of damaged elements. This crack propagates into the dam along the dam–foundation boundary. The nucleation of this crack is induced by the stress concentration in this area due to the infinitely rigid foundation. At this time, some partial tensile damage is also observed on several elements along the upstream face.

During the next large excursion in the upstream direction, at time t_3, a localized band of damaged elements forms near the downstream change of slope. As this downstream crack propagates toward the upstream direction, it curves down due to the rocking motion of the top block of the dam. The crack at the base of the dam is closed at time t_3 by the compressive stresses in this region. This is easily verified by looking at the contour plot of SDEG at time t_3, which clearly shows that the stiffness is recovered on this region, indicating that the crack is closed.

When the load is reversed, corresponding to the next excursion in the downstream direction at time t_4, the downstream crack closes and the stiffness is recovered on that region. At this time tensile damage localizes on several elements along the upstream face, leading to the formation of a horizontal crack that propagates toward the downstream crack.

As the upper block of the dam oscillates back and forth during the remainder of the earthquake, the upstream and downstream cracks close and open in an alternate fashion. The dam retains its overall structural stability since both cracks are never under tensile stress during the earthquake. The distribution of tensile damage at the end of the earthquake is shown in Figure 8 at time t_6. The contour plot of the stiffness degradation variable indicates that, except at the vicinity of the crack tips, all cracks are closed under compressive stresses and most of the stiffness is recovered. No compressive failure is observed during the simulation. The damage patterns predicted by Abaqus are consistent with those reported by other investigators.

Abaqus/Explicit results

Figure 9 shows the distribution of tensile damage at the end of the Abaqus/Explicit simulation. Two major cracks develop during the earthquake, one at the base of the dam and the other at the downstream change of slope. If we compare these results with those from the analysis in Abaqus/Standard (see Figure 8 at time t_6), we find that Abaqus/Standard predicted additional damage localization zones on the upstream face of the dam. The differences between the results are due to the effect of the dam–reservoir hydrodynamic interactions, which are included in the Abaqus/Standard simulation via an added-mass user element and are ignored in Abaqus/Explicit. This is easily verified by running an Abaqus/Standard analysis without the added-mass user element. The results from this analysis, shown in Figure 10, are consistent with the Abaqus/Explicit results in Figure 9 and confirm that additional damage to the upstream wall occurs when the hydrodynamic interactions are taken into account.

Input files

Abaqus/Standard input files

koyna_freq.inp

Frequency analysis of the Koyna dam.

koyna_std.inp

Seismic analysis of the Koyna dam, including hydrodynamic interactions.

koyna2_std.inp

Seismic analysis of the Koyna dam, not including hydrodynamic interactions.

koyna_haccel.inp

Transverse ground acceleration record.

koyna_vaccel.inp

Vertical ground acceleration record.

addedmass_uel.f

User subroutine `UEL` used by koyna_std.inp to model hydrodynamic interactions via the added mass technique.

koyna_std_to_xpl.inp

Analysis of the pre-seismic state of the Koyna dam. These results are imported by koyna_xpl.inp.

Abaqus/Explicit input files

koyna_xpl.inp

Seismic analysis of the Koyna dam, not including hydrodynamic interactions; requires import of the results from koyna_std_to_xpl.inp.

koyna_hp_vdload.f

User subroutine `VDLOAD` used by koyna_xpl.inp to specify hydrostatic pressure.

koyna2_xpl_std.inp

Analysis of the post-seismic state of the Koyna Dam; requires import of the results from koyna_xpl.inp.

References

Bhattacharjee, S. S., and P. Léger, "Seismic Cracking and Energy Dissipation in Concrete Gravity Dams," *Earthquake Engineering and Structural Dynamics*, vol. 22, pp. 991–1007, 1993.

Cervera, M., J. Oliver, and O. Manzoli, "A Rate-Dependent Isotropic Damage Model for the Seismic Analysis of Concrete Dams," *Earthquake Engineering and Structural Dynamics*, vol. 25, pp. 987–1010, 1996.

Chopra, A. K., and P. Chakrabarti, "The Koyna Earthquake and the Damage to Koyna Dam," *Bulletin of the Seismological Society of America*, vol. 63, no. 2, pp. 381–397, 1973.

Ghrib, F., and R. Tinawi, "An Application of Damage Mechanics for Seismic Analysis of Concrete Gravity Dams," *Earthquake Engineering and Structural Dynamics*, vol. 24, pp. 157–173, 1995.

Lee, J., and G. L. Fenves, "A Plastic-Damage Concrete Model for Earthquake Analysis of Dams," *Earthquake Engineering and Structural Dynamics*, vol. 27, pp. 937–956, 1998.

Westergaard, H. M., "Water Pressures on Dams during Earthquakes," *Transactions of the American Society of Civil Engineers*, vol. 98, pp. 418–433, 1933.

Tables

Table 1. Material properties for the Koyna dam concrete.

Young's modulus:	E = 31027 MPa
Poisson's ratio:	ν = 0.15
Density:	ρ = 2643 kg/m^3
Dilation angle:	ψ = 36.31°

Compressive initial yield stress:	σ_{c0} = 13.0 MPa
Compressive ultimate stress:	σ_{cu} = 24.1 MPa
Tensile failure stress:	σ_{t0} = 2.9 MPa

Table 2. Natural frequencies of the Koyna dam.

Mode	Natural Frequency (rad sec^{-1})	
	Abaqus	Chopra and Chakrabarti (1973)
1	18.86	19.27
2	49.97	51.50
3	68.16	67.56
4	98.27	99.73

Figures

Figure 1. Geometry of the Koyna dam.

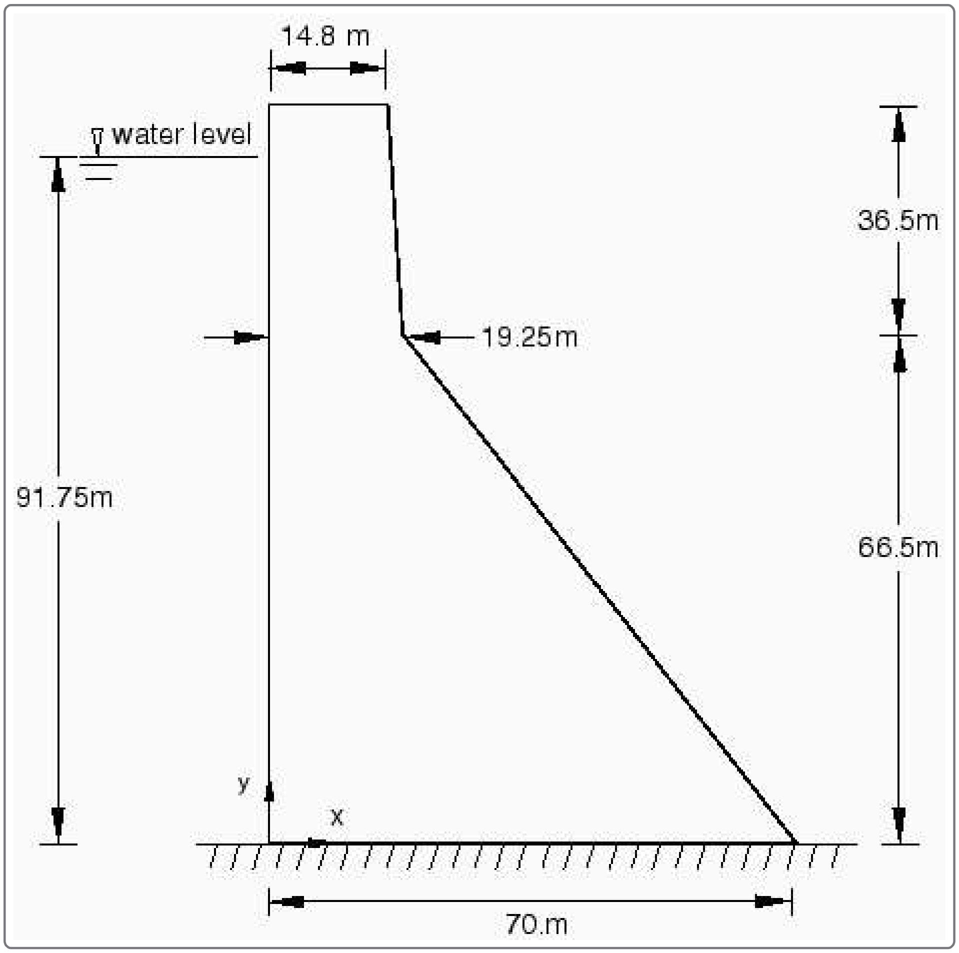

Figure 2. Finite element mesh.

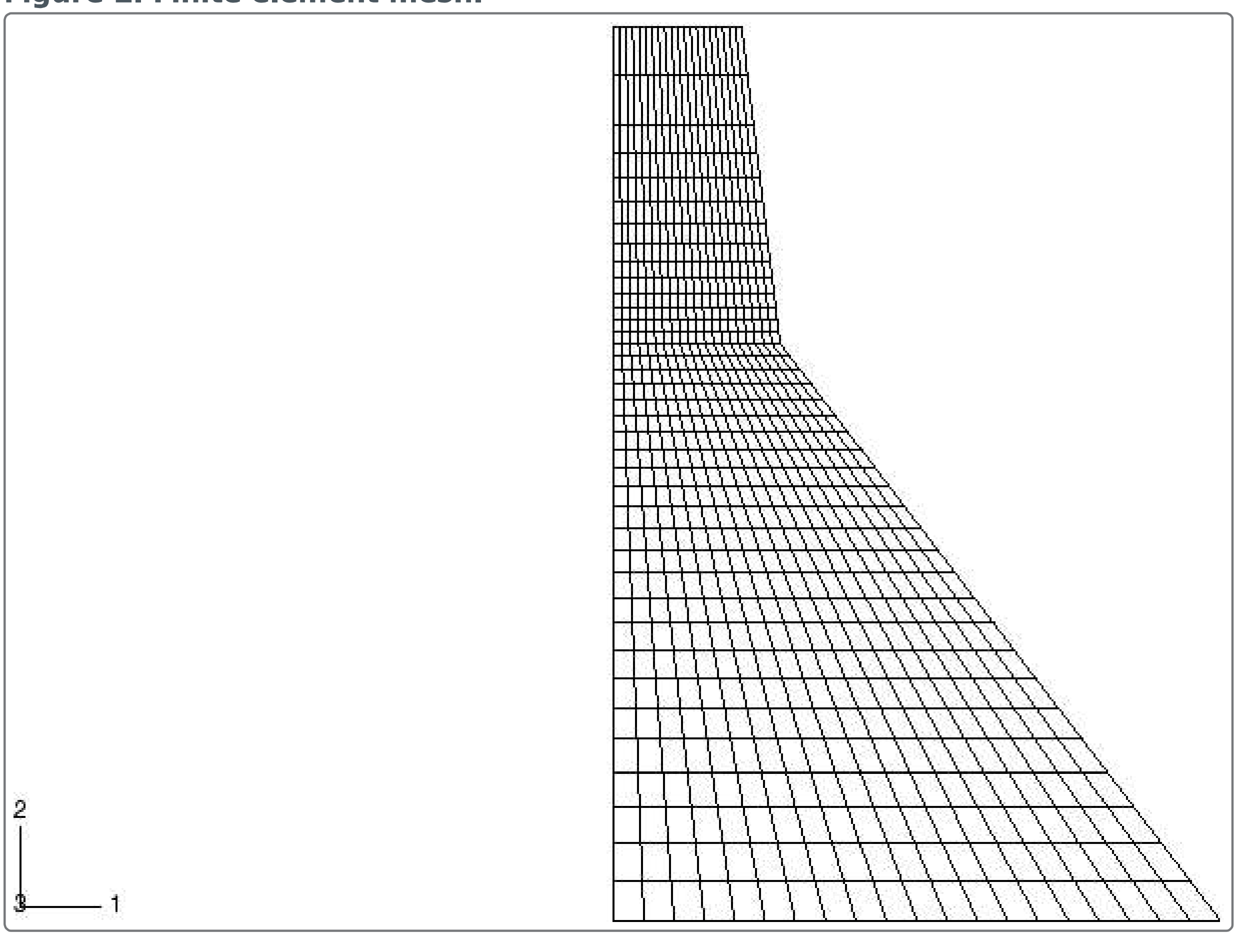

Figure 3. Koyna earthquake: (a) transverse and (b) vertical ground accelerations.

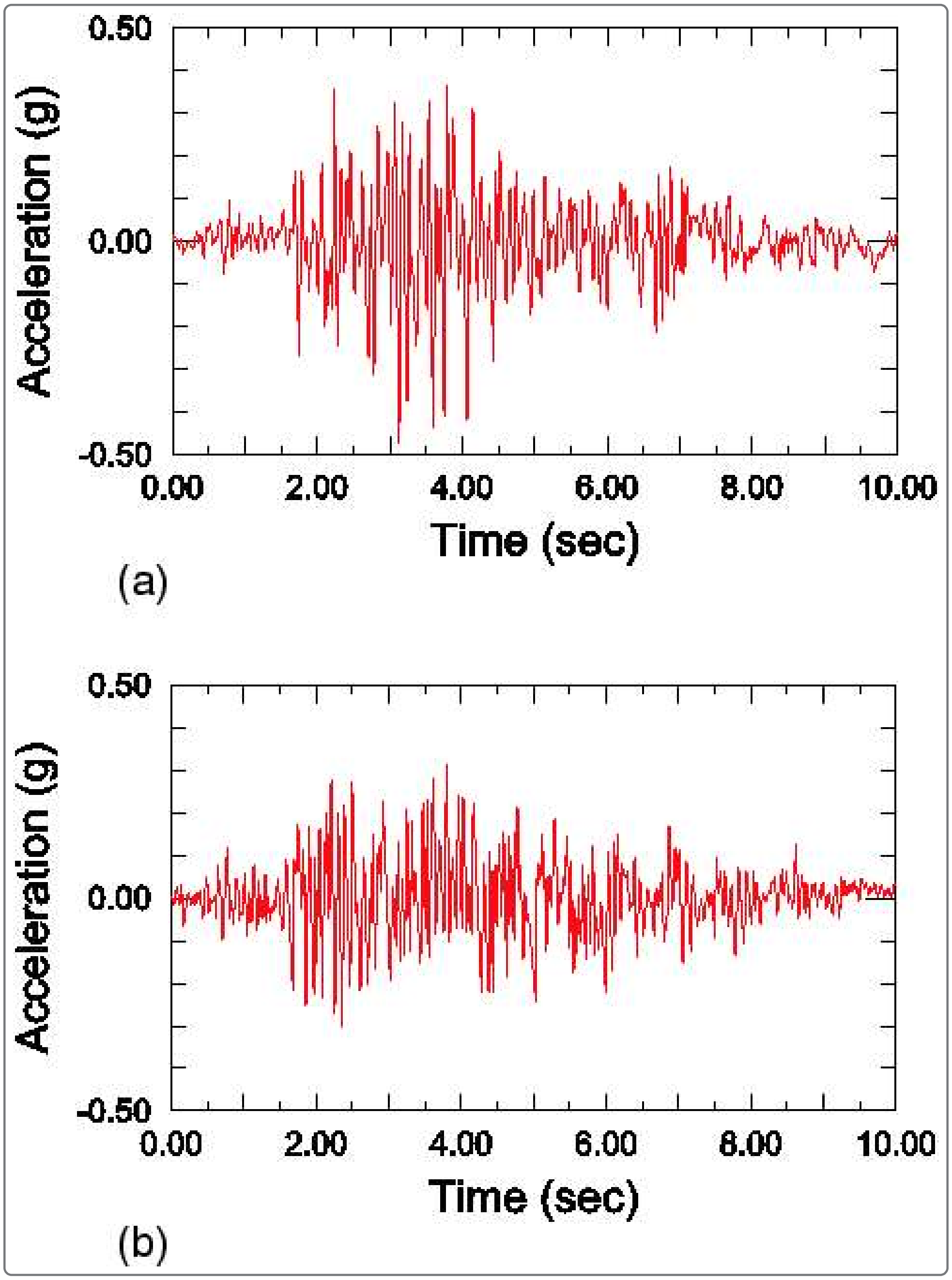

Figure 4. Concrete tensile properties: (a) tension stiffening and (b) tension damage.

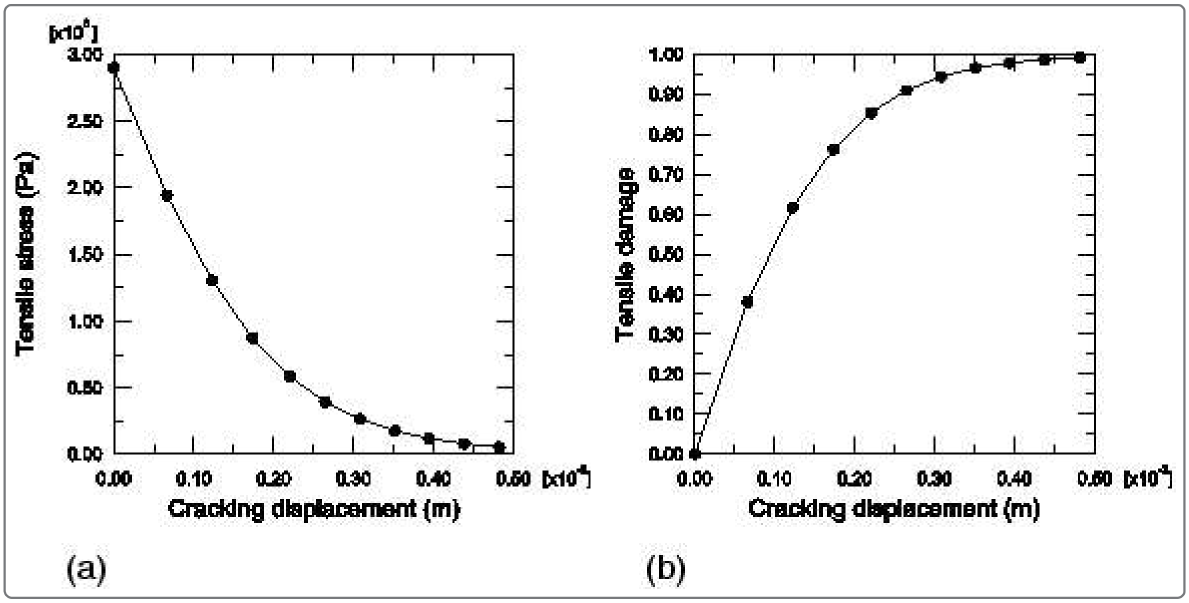

Figure 5. Horizontal crest displacement (relative to ground displacement).

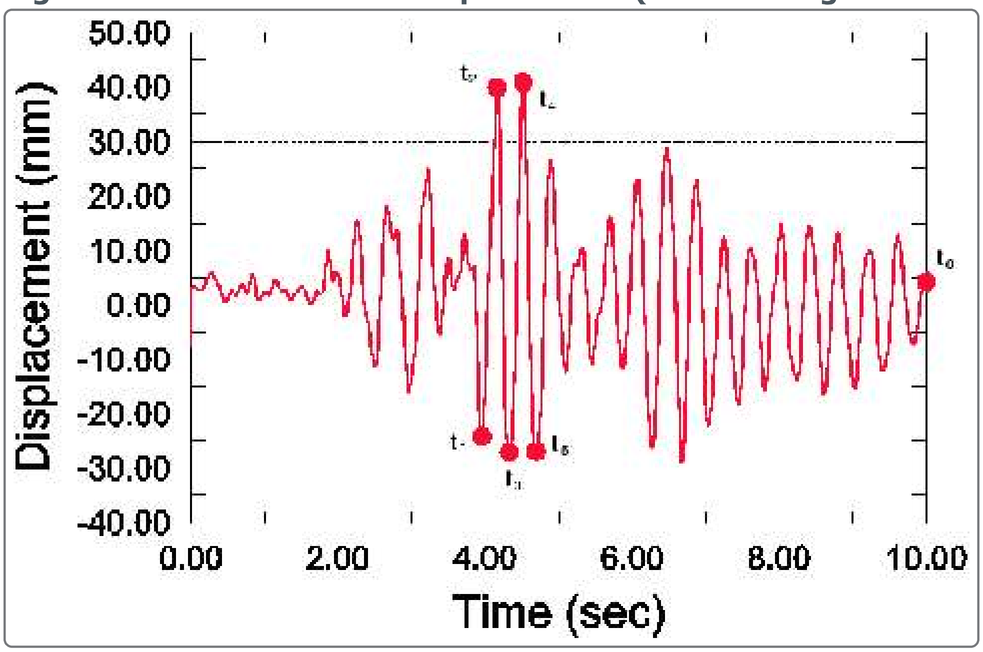

Figure 6. Evolution of tensile damage (Abaqus/Standard); deformation scale factor = 100.

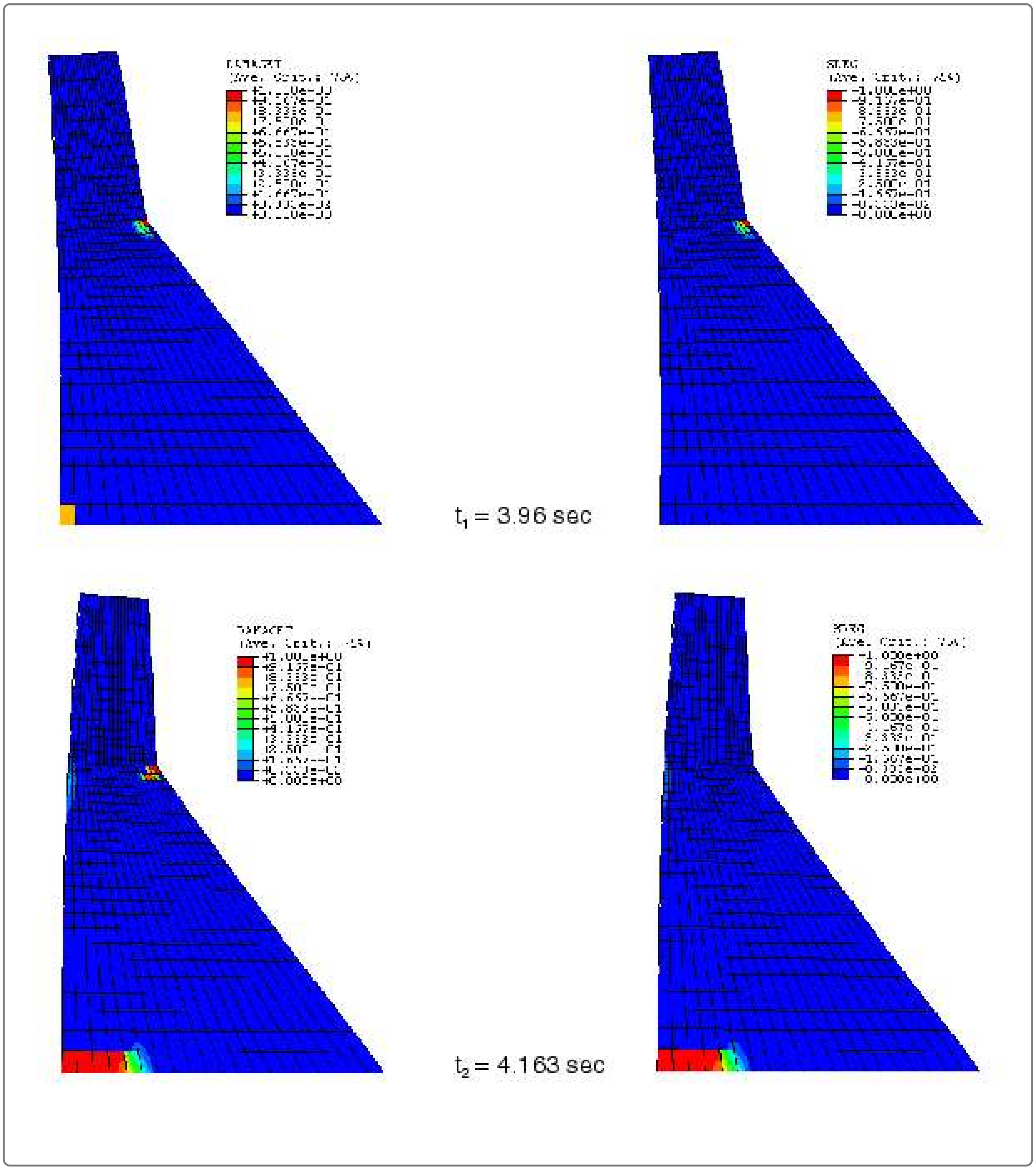

Figure 7. Evolution of tensile damage (Abaqus/Standard); deformation scale factor = 100.

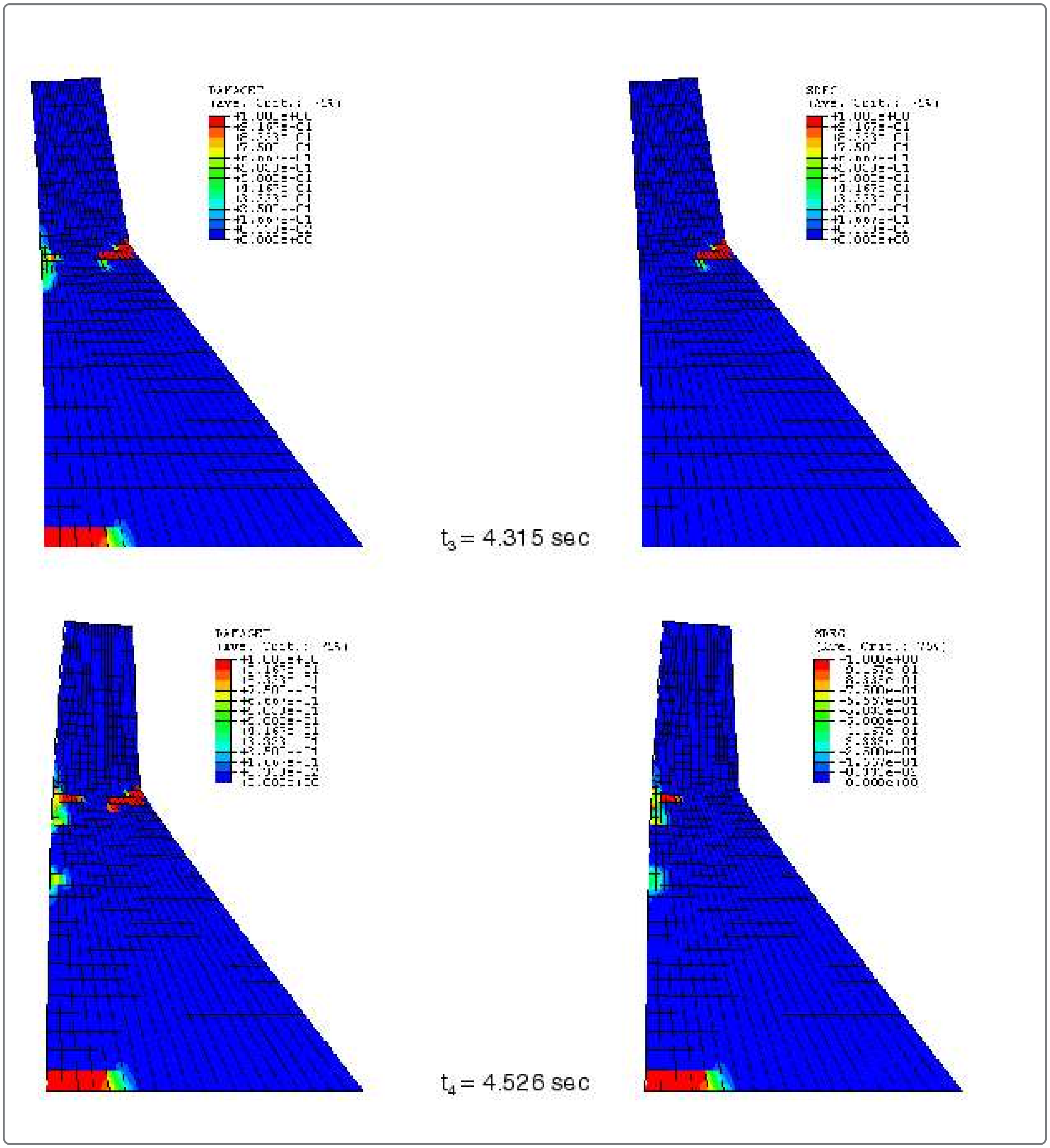

Figure 8. Evolution of tensile damage (Abaqus/Standard); deformation scale factor = 100.

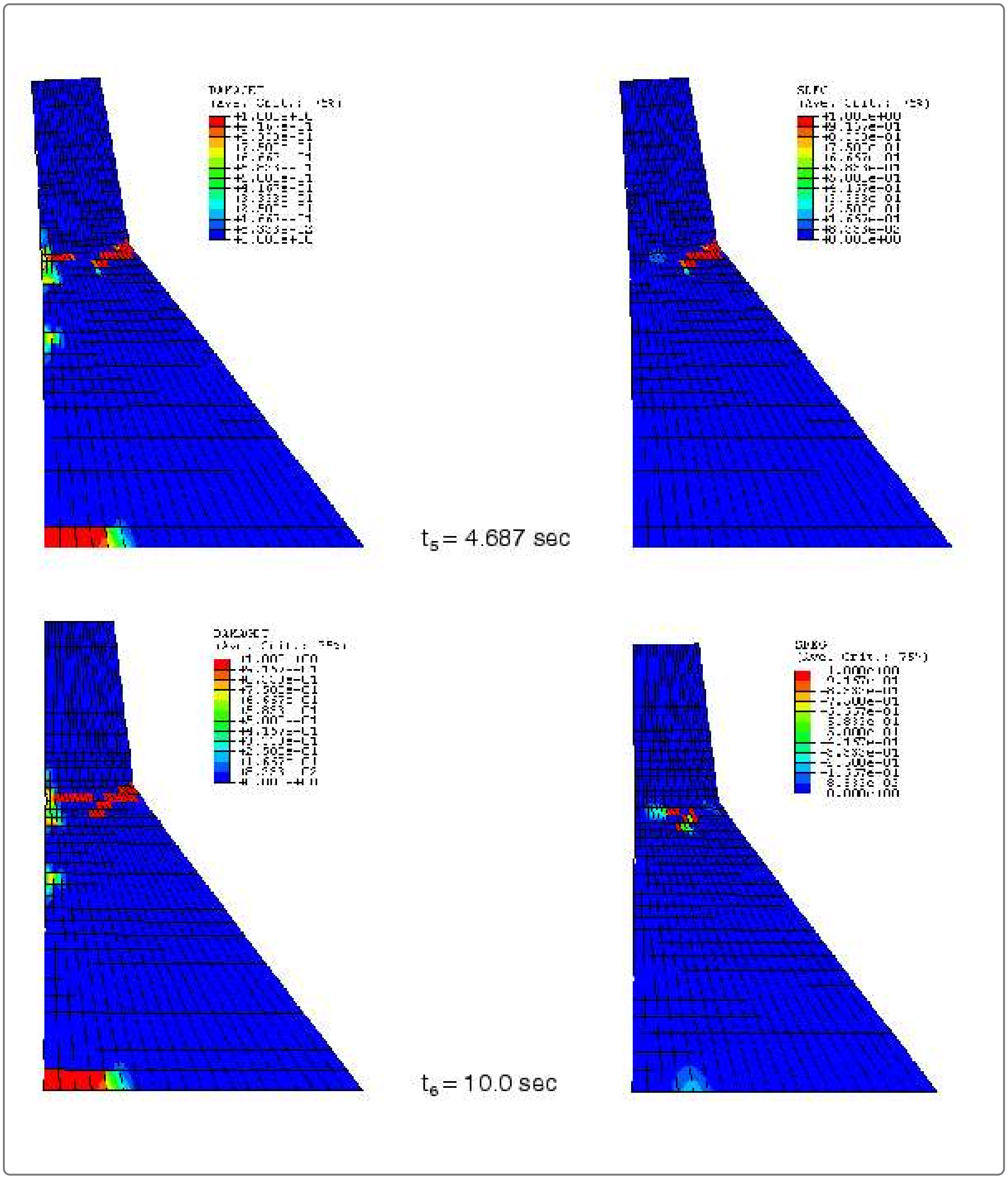

Figure 9. Tensile damage at the end of the Abaqus/Explicit simulation without dam–reservoir hydrodynamic interactions; deformation scale factor = 100.

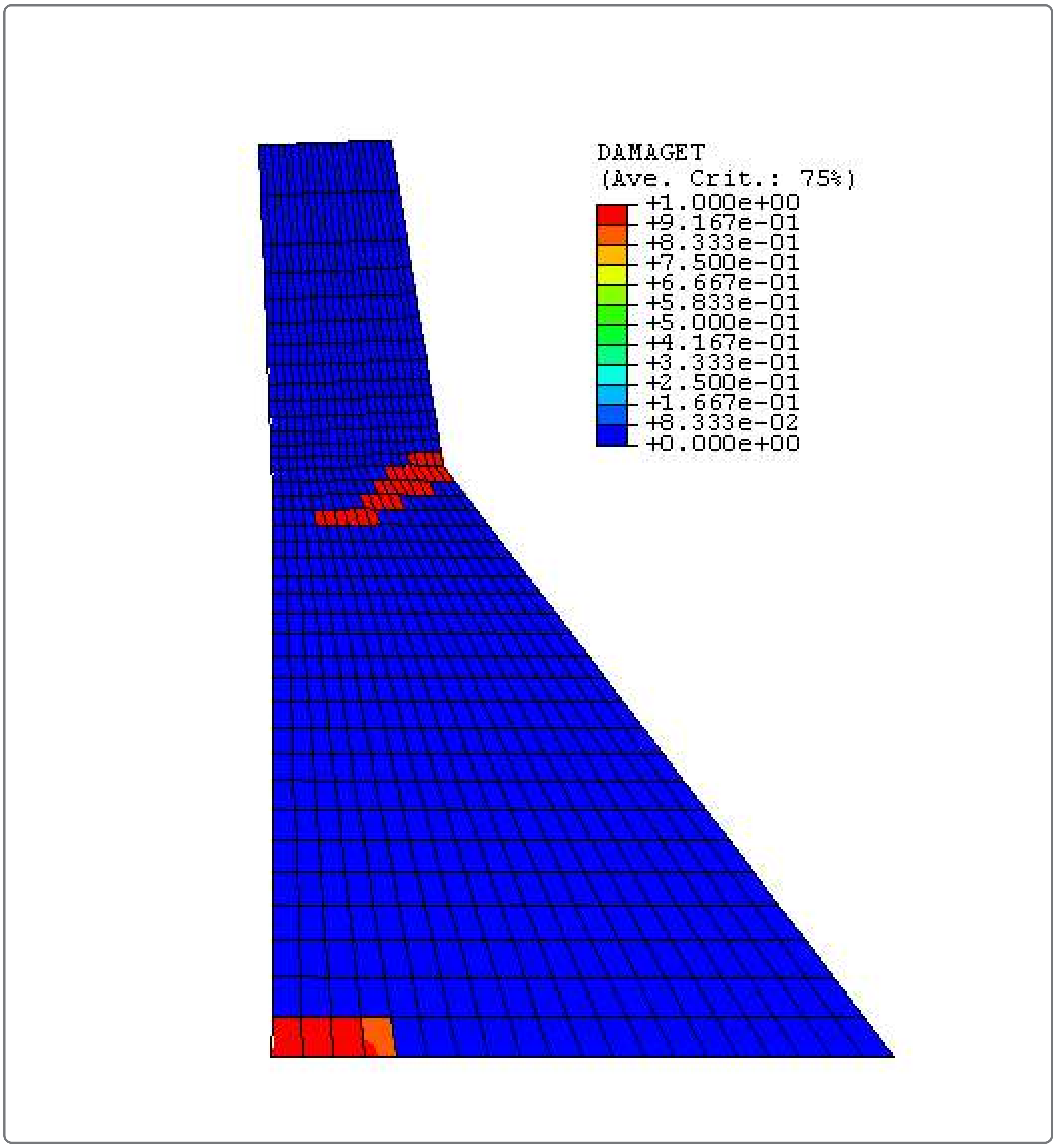

Figure 10. Tensile damage at the end of the Abaqus/Standard simulation without dam–reservoir hydrodynamic interactions; deformation scale factor = 100.

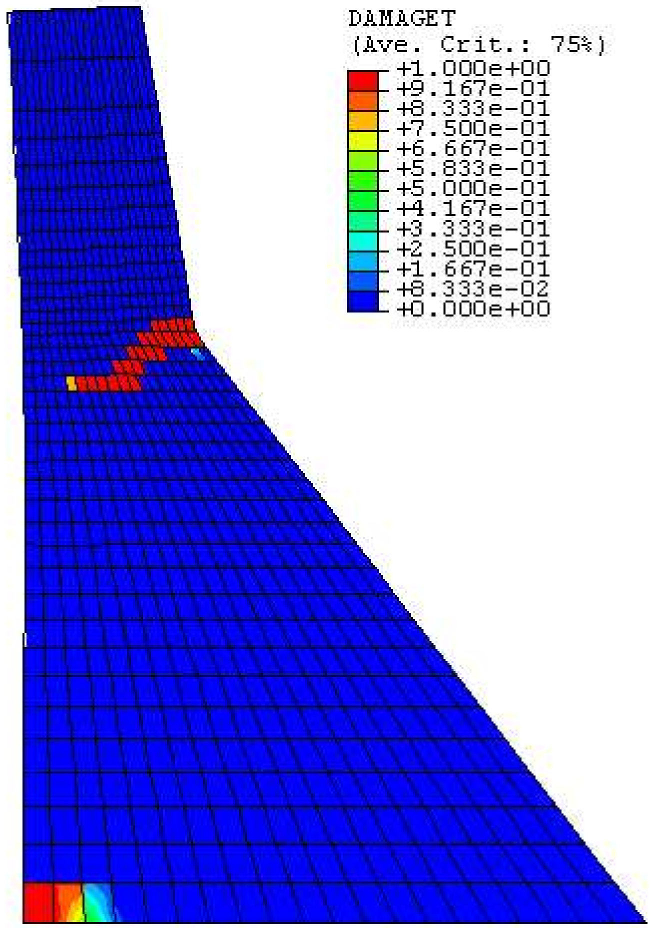
DAMAGET
(Ave. Crit.: 75%)
+1.000e+00
+9.167e-01
+8.333e-01
+7.500e-01
+6.667e-01
+5.833e-01
+5.000e-01
+4.167e-01
+3.333e-01
+2.500e-01
+1.667e-01
+8.333e-02
+0.000e+00